COUPLED THERMO-MECHANICAL FEM ANALYSIS OF TWIST COMPRESSION DEFORMATION PROCESS①

Xue Kemin, Zhang Zhengrong, Xia Yongjiang, Lu Yan
Metal Forming Division, # 435, Harbin Institute of Technology, Harbin 150001

ABSTRACT 3-D rigid-viscoplastic FEM of compressible materials was applied to analyze the deformation behavior during twist-compression forming of axisymmetrical body at high temperatures. When calculating the temperature fields, considering the thermo-mechanical coupling effect between temperature and deformation, 2-D FEM and CNG methods were adopted, and the up-winding technique was used to avoid the influences of numerical instability on calculated results.

Key words twist-compression rigid-viscoplastic FEM thermo-mechanical coupling

1 INTRODUCTION

Upsetting is one of the most common forging techniques, but the friction between billet and tool will greatly spoil the quality of the forging pieces. However, twist-compression forming, in which a billet is exerted a twisting torque on the cross-sectional plane during upsetting, can greatly improve the quality of the forging pieces.

In plastic working, especially in hot working process, temperature is one of the most important factors to be considered. So a comprehensive study on the relations between temperature and deformation and applying thermo-mechanical coupling FEM to analyze plastic working will be of great significance both in theory and practice. Based on the past achievements, the authors applied 3-D rigid-viscoplastic FEM of compressible materials to systematically study and analyze the twist compression forming process.

2 VISCO-PLASTICAL CONSTITUTIVE RELATION AND VARIATIONAL PRINCIPLE

Plastic working is highly non-linear. Now some approximate viscoplastic constitutive models have been used commonly. In this study, the authors adopt the super stress model together with considering the thermo-mechanical coupling effects. This model can be expressed as follows:

$$\sigma_e = Y(T)\,\alpha(\bar{\varepsilon})\left(1+\left(\frac{\dot{\bar{\varepsilon}}}{r}\right)^n\right) \tag{1}$$

where σ_e is the effective stress or flow stress, $Y(T)$ is the initial yielding stress dependent on temperature, $\bar{\varepsilon}$ and $\dot{\bar{\varepsilon}}$ are the effective strain and the effective strain rate, r and n are the constants dependent on material.

In this analysis, we assume that the material obeys the Levy-Mises criteria namely

$$\sigma'_{ij} = \frac{2}{3}\frac{\dot{\varepsilon}_{ij}}{\dot{\bar{\varepsilon}}_e}\sigma_e \tag{2}$$

If the analysed material in visco-plastic FEM is compressible, σ_e and $\dot{\bar{\varepsilon}}_e$ can be obtained from

$$\sigma_e = \left(\frac{3}{2}\sigma'_{ij}\sigma'_{ij} + g\sigma_m^2\right)^{1/2} \tag{3}$$

$$\dot{\bar{\varepsilon}}_e = \left(\frac{3}{2}\dot{\varepsilon}_{ij}\dot{\varepsilon}_{ij} + \frac{1}{g}\dot{\varepsilon}_v^2\right)^{1/2} \tag{4}$$

where g is volume compressible coefficient.

The components of the strain rate tensor $\dot{\varepsilon}_{ij}$ can be obtained through eq. (5) under the condition of known deformation rate of every node

$$\dot{\varepsilon}_{ij} = [B]\{a\} \tag{5}$$

where $[B]$ is strain tensor matrix, and $\{a\}$ is a column matrix of deformation velocity.

① Received Nov. 6, 1996; accepted Mar. 12, 1997

Deformation velocity of each node can be obtained from the optimization of the energy functional given below

$$\prod = \int_V E(\dot{\varepsilon})\,dv - \int_\Gamma \boldsymbol{F}\,\boldsymbol{V}\,dT + \int_\Gamma \tau_i \mid \Delta v \mid dt - \int_\Gamma \tau_i v_D\,dv \quad (6)$$

where Γ is boundary surface, V is the volume of deformation zone, $\mid \Delta v \mid$ is the relative velocity between tool and billet, and v_D is the twist velocity of tool.

In eq. (6), the first item ($\int_V E(\dot{\varepsilon})\,dv$) is the consumed energy by plastic deformation, the second item($\int_\Gamma \boldsymbol{F}\boldsymbol{V}dT$) is the energy produced by axial pressure, the third item($\int_\Gamma \tau_i \mid \Delta v \mid dt$) is the consumed energy by friction, and the last item ($-\int_\Gamma \tau_i V_D\,dv$) is the energy produced by active friction between tool and billet, but this item is zero in common upsetting.

Through solving eq. (6), we may obtain true velocity field, and then any mechanical variation at any time may be obtained through solving the above equations.

3 TEMPERATURE FIELD AND THERMAL CONDUCTION

In actual plastic working, thermal conduction is very complicated and unstable. In this paper, according to Flour's heat conduction law, the temperature field can be written as

$$\nabla^{\mathrm{T}}(k\,\nabla T) + q = \rho C_p \partial T/\partial t \quad (7)$$

where $\nabla = \{\partial/\partial x + \partial/\partial y + \partial/\partial z\}^{\mathrm{T}}$; k, ρ and C_p are the heat conduction coefficient, the material density and the specific heat respectively, and they may be different in billet and die; q is the internal heat generation, it should be zero in die but depend on plastic deformation energy in billet and can be expressed by

$$q = \beta E(\dot{\varepsilon}) \quad (8)$$

where β is a coefficient whose value is 0.9~0.95.

Initial condition and boundary conditions such as convection, known heat flow and known temperature condition in eq. (7) can be written as

$$k\partial T/\partial n = -h(T - T_0) \quad (9)$$

$$k\partial T/\partial n = -q_s \quad (10)$$

$$T = \overline{T} \quad (11)$$

$$q_s = \int_{S_p} \tau_i \mid \Delta v \mid d\Gamma \quad (12)$$

where n is a coordinate normal to the surface, h is the heat conduction coefficient, T_0 and $\overline{T}$ are the ambient temperature and the known boundary temperature, q_s is the heat flow density which is heat energy produced by friction. In the empirical model, all the work of friction will be turned into heat which is separated into two parts seperatively flowing into the billet and the tool. They can be given by

$$q_{ds} = \eta_1 q_s \quad (12a)$$

$$q_{bs} = \eta_2 q_s \quad (12b)$$

Where q_{bs} and q_{ds} are the heat flowing into the billet and the die, η_1 and η_2 are coefficients which can be obtained through

$$\eta_1 = \frac{(K_1/\rho_1 C_1)^{1/2}}{(K_1/\rho_1 C_1)^{1/2} + (K_2/\rho_2 C_2)^{1/2}},$$

$$\eta_2 = \frac{(K_2/\rho_2 C_2)^{1/2}}{(K_1/\rho_1 C_1)^{1/2} + (K_2/\rho_2 C_2)^{1/2}}$$

where K_1 and K_2 are the heat conduction coefficients of the die and the billet, ρ_1 and ρ_2 are the densites of the die and the billet, C_1 and C_2 are the specific heats of the die and the billet.

To sum up, eq. (7) can be expressed as

$$\prod(T) = \int_V [\nabla^{\mathrm{T}}(k\,\nabla T) - q_v T + \partial T/\partial t T]\,dV + \int_{\Gamma_1} h(T - T_0)\,d\Gamma_1 + \int_{\Gamma_2} q_s T\,d\Gamma_2 \quad (13)$$

where V is the volume of the studied object, Γ_1 and Γ_2 are the boundary surfaces.

4 FINITE ELEMENT SIMULATION AND RESULTS ANALYSIS

In twist-compression deformation, when plastic deformation work and frictional heat calculated in 3-D FEM are served as the inner heat source of a 2-D temperature field, they must be changed. In addition, the inner heat source doesn't exist in the die.

When applying the FEM to analyze the temperature field, eq. (13) could be expressed by column matrix

$$[K]\{T\} + [C]\frac{\partial\{T\}}{\partial t} = \{P_0\} \quad (14)$$

where $[K]$ is a heat conduction matrix, representing the conduction peculiarity of temperature field; $[C]$ is a matrix of specific heat, namely changing temperature matrix, showing heat capacitance peculiarity; $[P_0]$ is a column matrix representing the heat produced from the inner heat source and exchanged through the boundaries.

The authors adopt Galerkin equation to solve the following differential equation

$$2\frac{\partial[T]^t}{\partial t} + \frac{\partial[T]^{t-\Delta t}}{\partial t} = \frac{3}{\Delta t}([T]^t - [T]^{t-\Delta t}) \quad (15)$$

From eqs. (14) and (15), we can derive an equation

$$(2[K] + \frac{3[C]}{\Delta t})\{T\}^t = 2\{P_0\}^t + \{P_0\}^{t-\Delta t} + (\frac{3[C]}{\Delta t} - [K])[T]^{t-\Delta t} \quad (16)$$

When solving this equation in high deformation speed, the convection item in heat conduction equation will make resolutions instable, which can be avoided through adopting the upwinding method.

The authors use the own-developed program to simulate the twist compression deformation processes of different parameters.

Fig. 1 shows the grids of workpiece after twist compression deformation, which indicates that the grids have produced some distortion, the original axial section doesn't keep plane any more, and the change of axial and radial directions is non-linear. The tangent displacement of the upper part near the die is gradually dropped after appearing a maximum value in the radial direction and has a smaller value in the outer circle. This is because the contact friction along the radial direction gradually drops, the relative mobile velocity gradually increases between the die and the billet, and the radial change rate of the tangent displacement relatively drops. In axial direction, the tangent displacement of the upper part of the billet has a greater value but drops fast, and that of the medium part has a smaller value. This indicates that the shear stress produced by the active friction has a great effect on the deformation of the upper part, but has little effect on the medium part. This also shows that the existence of the shear stress makes the grids of the deformation body little distorted and so the deformation is very homogeneous.

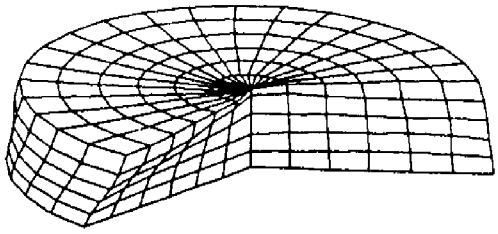

Fig. 1 Grids of workpiece after twist-compression forming
($H_0/D_0 = 0.5$, $\mu = 0.2$, $\varepsilon_z = 0.33$, $\omega = 15°$, $t = 25$ s)

Fig. 2 shows the isograms of various variations, which indicates that although the effective strain is still small in the twist compression deformation and its value has little difference from upsetting, the homogeneity of deformation is greatly improved. It can be seen from the distribution of temperature that the temperature of the center of the deformation body is very high, which is because the great deformation of the center part produces a great deal of heat, and also because the speed of the heat conduction is very slow . The radial temperature gradient in the center is very larger than those in the ends, moreover, its isopleth gradually winds up, which shows the outer circle near the contact surface suffers a great deformation and the effect of the frictional heat. Seen from the distribution of the effective stress, the deformation is small. This results from the common action of the temperature and the strain rate, but the former affects less than the later.

Figs. 3, 4 and 5 respectively show the distribution of some variations under different conditions. Fig. 3 is the isogram in the middle of the process and different from the strain rate distribution in Fig. 2, which shows that the process is non-linear. With the development of deformation, the shear deformation becomes more obvi-

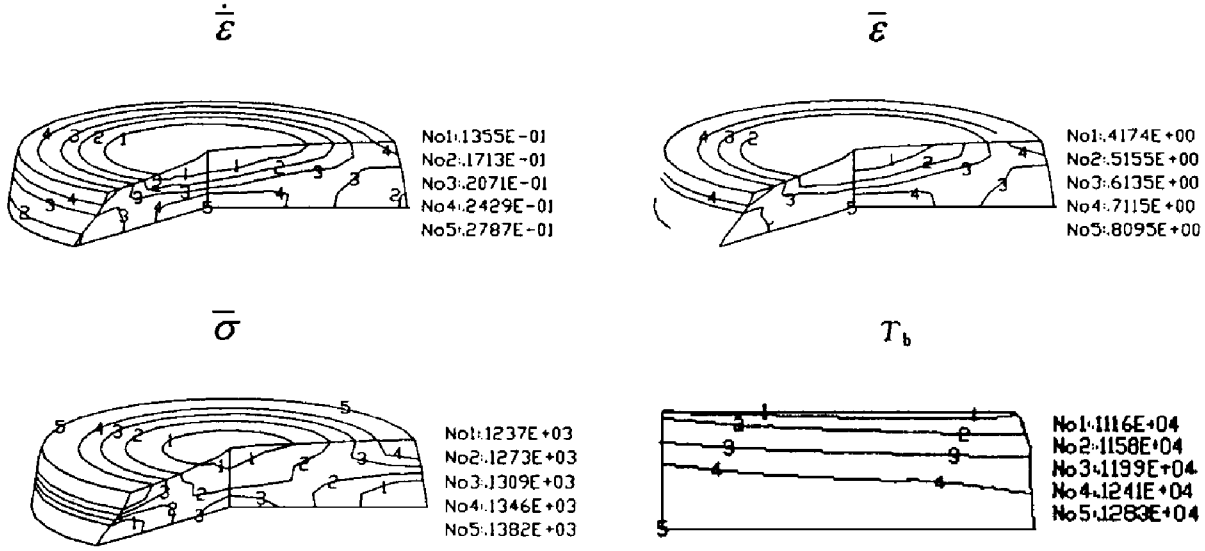

Fig. 2 Isograms of various variations in twist-compression
(H_0/D_0= 0.5, μ= 0.2, ε_z= 33%, ω= 15°, t = 25 s, T_d= 698 K)

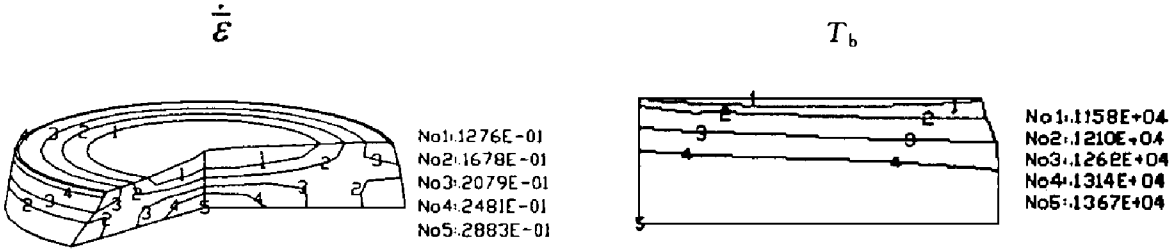

Fig. 3 Isograms of some variations in twist-compression
(H_0/D_0= 0.5, μ= 0.2, ε_z= 16.7%, ω= 7.5°, t= 12.5 s, T_d= 698 K)

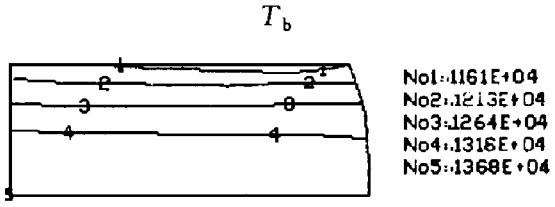

Fig. 4 Isograms of workpiece temperature in twist-compression
(H_0/D_0= 0.5, μ= 0.5, ε_z= 33%, ω= 30°, t= 12.5 s, T_d= 698 K)

ous, and the distribution of the effective strain rate becomes more homogeneous. Because of little heat conduction of the center to the die in a short time, so the axial temperature gradient changes greatly. At this time, a great deformation happens both in the center and the outer circle near the contact surface, and the gradient of the strain rate also becomes great, which shows the effect of the temperature on the deformation. In Fig. 4, when raising the deformation rate, the twist angle velocity and the frictional factor, the time of deformation correspondingly dropped. Moreover, as the heat produced by the

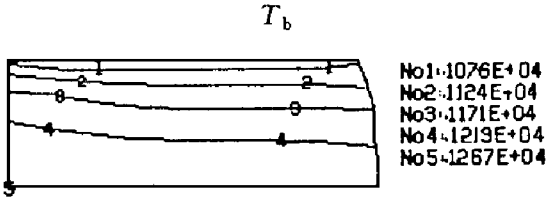

Fig. 5 Isograms of workpiece temperature in twist-compression
(H_0/D_0= 0.5, μ= 0.5, ε_z= 33%, ω= 15°, t= 25 s, T_d= 298 K)

friction and the plastic working increases, the temperature in Fig. 4 is a little higher than that in Fig. 2. Fig. 5 shows that the low temperature of the die makes the heat in the billet transfer fast, the temperature gradient changes greatly, and the temperature of the contact surface drops.

5 CONCLUSIONS

The above results show that, during the twist compression deformation, both the strain rate and the temperature affects the deformation. The increment of the strain rate can increase the power of the plastic working, and then raise the temperature of deformation body, which reversibly affects the next deformation. The frictional heat and the exchanged heat among the deformation body , the die and the surroundings affect not only the temperature of the deformation body, but also the whole deformation process. So applying the rigid viscoplastic FEM to simulate the twist compression deformation can comprehensively consider the influence of the temperature and the strain rate, make results more suitable to the practice, efficiently explain the act of the shear stress on the deformation and analyze the influences of many parameters on the whole deformation process more systematically and completely.

REFERENCES

1 Xue K M and Lu Y. In: Proceedings of the 4th ICTP. Beijing: International Academic Publisher, 1993: 1065– 1070.
2 Xue K M and Lu Y. Journal of Mechanics and Engneering, 1996, 32(1): 74– 78.
3 Hong S Z and Dong D F. Journal of Mechanics and Engineering, 1996, 32(1): 62– 67.
4 Liu G D. Numerical Simulation of Temperature Fields. Chongqing: Chongqing University Publisher, 1990: 70– 105.
5 Lin Zongqing, Chen Changcheng. Journal of Materials Processing Technology, 1995, 49: 125– 147.
6 Kelly W and Nakazawa S *et al*. Int J Num Math Eng, 1980, 15: 1705– 1711.

(Edited by Peng Chaoqun)